Inorg. Chem. **2007**, *46*, 2627–2636

New Bonding Modes for Boraamidinate Ligands in Heavy Group 15 Complexes: Fluxional Behavior of the 1:2 Complexes, LiM[PhB(N^{t}Bu)$_2$]$_2$ (M = As, Sb, Bi)

Jari Konu, Maravanji S. Balakrishna,‡ Tristram Chivers,* and Thomas W. Swaddle

Department of Chemistry, University of Calgary, Calgary, Alberta, Canada T2N 1N4

Received November 30, 2006

The reactions of MCl_3 with $Li_2[PhB(N^tBu)_2]$ in 1:1, 1:1.5, and 1:2 molar ratios in diethyl ether produced the monoboraamidinates $ClM[PhB(N^tBu)_2]$ (**1a**, M = As; **1b**, M = Sb; **1c**, M = Bi), the novel 2:3 boraamidinate complexes $[PhB(N^tBu)_2]M$-μ-$N(^tBu)B(Ph)N(^tBu)M[PhB(N^tBu)_2]$ (**2b**, M = Sb; **2c**, M = Bi), and the bisboraamidinates $LiM[PhB(N^tBu)_2]_2$ (**3a**, **3a**·OEt_2, M = As; **3b**, M = Sb; **3c**·OEt_2, M = Bi), respectively. The 2:3 complexes **2b** and **2c** were also observed in the reactions carried out in a 1:2 molar ratio at room temperature. All complexes have been characterized by multinuclear NMR spectroscopy (^{1}H, ^{7}Li, ^{11}B, and ^{13}C) and by single-crystal X-ray structural determinations. The molecular units of the mono-boraamidinates **1a**–**c** are isostructural, but their crystal packing is distinct as a result of stronger intermolecular close contacts going from **1a** to **1c**. In the novel 2:3 bam complexes **2b** and **2c**, each metal center is N,N′-chelated by a bam ligand and these two $[M(bam)]^+$ units are bridged by the third $[bam]^{2-}$ ligand. The structures of the unsolvated bis-boraaminidate complexes **3a** and **3b** consist of $[Li(bam)]^-$ and $[M(bam)]^+$ monomeric units linked by Li–N and M–N bonds to give a tricyclic structure. Solvation of the Li^+ ion by diethyl ether results in a bicyclic structure composed of four-membered BN_2As and six-membered BN_3AsLi rings in **3a**·OEt_2. In contrast, the analogous bismuth complex **3c**·OEt_2 exhibits a tetracyclic structure. Variable-temperature NMR studies reveal that the nature of the fluxional behavior of **3a**–**c** in solution is dependent on the group 15 center.

Introduction

The dianionic boraamidinate (bam) ligand is formally isoelectronic with the extensively studied monoanionic amidinate (am) ligand. The first bam metal complex, a dimeric tin(II) boraamidinate, was reported in 1979. It was obtained in low yield from the reaction of $Li[N(BMe_2)(SiMe_3)]$ with $SnCl_2$.[1] Dilithio boraamidinates were introduced as reagents for the synthesis of metal complexes in 1990.[2,3] Although the use of these reagents in metathesis represents by far the most general and versatile route to a wide range of main group and transition metal systems, their solid-state structures were not established until 2000.[4]

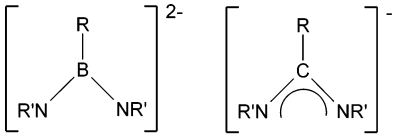

Recent work on early main group and transition-metal complexes has established that the 2− charge on the bam ligand results in some interesting fundamental differences compared to behavior of the monoanionic am ligand. One intriguing consequence is the facile tendency for redox transformations involving the oxidation of the $[bam]^{2-}$ dianion to the corresponding monoanion radical $[bam]^{-\bullet}$. This paramagnetic ligand can be stabilized through complexation to early main group metals.[5,6] In some cases it has been possible to isolate *stable* neutral radicals, for example the

* To whom correspondence should be addressed. Telephone: (403) 220-5741. Fax: (403) 289-9488. E-mail: chivers@ucalgary.ca.

‡ Permanent address: Department of Chemistry, Indian Institute of Technology, Bombay, Mumbai, India 400 076.

(1) Fusstetter, H.; Nöth, H. *Chem. Ber.* **1979**, *112*, 3672.
(2) Heine, A.; Fest, D.; Stalke, D.; Habben, C. D.; Meller, A.; Sheldrick, G. M *J. Chem. Soc., Chem. Commun.* **1990**, 742.
(3) Fest, D.; Habben, C. D.; Meller, A.; Sheldrick, G. M.; Stalke, D.; Pauer, F. *Chem. Ber.* **1990**, *123*, 703.
(4) Brask, J. K.; Chivers, T.; Schatte, G. *Chem. Commun.* **2000**, 1805.
(5) Chivers, T.; Eisler, D. J.; Fedorchuk, C.; Schatte, G.; Tuononen, H. M.; Boeré, R. T. *Chem. Commun.* **2005**, 3930.
(6) Chivers, T.; Eisler, D. J.; Fedorchuk, C.; Schatte, G.; Tuononen, H. M.; Boeré, R. T. *Inorg. Chem.* **2006**, *45*, 2119.

10.1021/ic0622757 CCC: $37.00
Published on Web 02/28/2007

Scheme 1. Bonding Modes for the Different Classes of bam Complexes[8] [a]

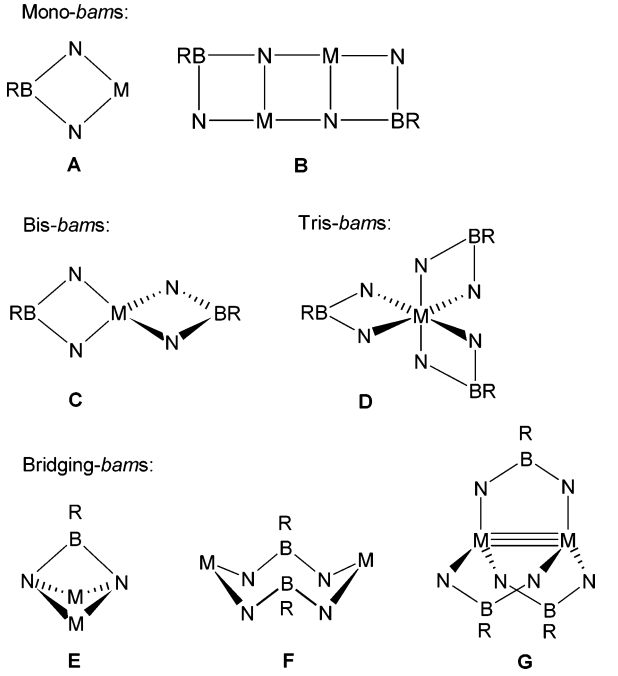

[a] Substituents on N are omitted for clarity.

spirocyclic systems $\{M[PhB(\mu\text{-}N^tBu)_2]_2\}^\bullet$ (M = Al, Ga).[5,6] The 2− charge also lowers the requirement for ancillary ligands around high oxidation state metal centers. Consequently, homoleptic species of the type $[ML_2]^{x-}$ (x = 0, 1, 2) and $[ML_3]^{2-}$ (L = bam) are common features of main group and transition metal complexes.[7−9]

The versatile coordination ability of the bam ligand is illustrated by the diversity of complexes that have been established to date for this bidentate ligand (Scheme 1). The N,N′-chelating mode, in which both nitrogen centers are three-coordinate, is observed for homoleptic mono-, bis- and tris-boraamidinates (**A**, **C**, and **D**). In the case of mono-boraamidinates, dimerization may occur with the formation of one four-coordinate nitrogen center (**B**). The bam ligand may also function in a bridging mode between two metal centers with both nitrogen atoms four-coordinate (**E**). Also, two bam ligands, in which both nitrogens are three-coordinate,
may bridge two metal centers (**F**). This arrangement can be considered to be an alternative to the dimeric structure **B**. Finally, it has recently been shown that three N,N′-chelating bam ligands may also bridge an M≡M unit (**G**, M = Mo, W).[10]

A survey of the literature of bam complexes of p-block elements reveals that most attention has been accorded to groups 13,[5,9,11] 14,[1−3,12−16] and 16.[17−19] For the group 15 elements, only phosphorus derivatives have been reported,[20,21] all of which fall under the category of mono-boraamidinates that adopt bonding mode **A**. The purpose of this investigation was to explore the coordination behavior of the bam ligand in complexes of the heavier group 15 elements and, especially, to assess the stereochemical influence of the lone pair on the main group metal center in the structures of the bis-bam complexes $Li[M(bam)_2]$ (M = As, Sb, Bi). In this paper, we describe the syntheses, solid-state structures, and spectroscopic characterization of the mono-boraamidinates $ClM[PhB(N^tBu)_2]$ (**1a**, M = As; **1b**, M = Sb; **1c**, M = Bi), the 2:3 bam complexes $[PhB(N^tBu)_2]M\text{-}\mu\text{-}N(^t\text{Bu})B(Ph)N(^t\text{Bu})\text{-}M[PhB(N^tBu)_2]$ (**2b**, M = Sb; **2c**, M = Bi), and the bis-boraamidinates $LiM[PhB(N^tBu)_2]_2$ (**3a**, **3a**·OEt_2, M = As; **3b**, M = Sb; **3c**·OEt_2, M = Bi). The nature of the fluxional behavior of **3a**−**c** in solution has been probed by variable-temperature NMR studies.

Experimental Section

General Procedures. All reactions and the manipulations of products were performed under an argon atmosphere using standard Schlenk techniques or in an inert atmosphere glove box. The compounds $PhBCl_2$ (Aldrich, 97%), $AsCl_3$ (Alfa, 99%), and $BiCl_3$ (Strem, 99.9%) were used as received. $SbCl_3$ (Aldrich, 99%) was sublimed prior to use. $LiN(H)^tBu$ was prepared by the addition of ^{n}BuLi to a solution of anhydrous ^{t}BuNH$_2$ in *n*-hexane at −10 °C, and its purity was checked by ^{1}H NMR spectroscopy. The compounds $PhB[N(H)^tBu]_2$ and $Li_2[PhB(N^tBu)_2]$ were prepared using literature methods.[21] The solvents *n*-hexane, toluene, Et_2O, and THF were dried by distillation over Na/benzophenone under a nitrogen atmosphere prior to use.

Spectroscopic Methods. The ^{1}H, ^{7}Li, ^{11}B, and ^{13}C NMR spectra were obtained in THF-d_8 or toluene-d_8 at 23 °C on a Bruker DRX 400 spectrometer operating at 399.59, 155.30, 128.20, and 100.49 MHz, respectively. ^{1}H and ^{13}C spectra are referenced to the solvent signal, and the chemical shifts are reported relative to $(CH_3)_4Si$. ^{7}Li and ^{11}B NMR spectra are referenced externally, and the chemical shifts are reported relative to a 1.0 M solution of LiCl in D_2O and to a solution of BF_3·Et_2O in C_6D_6, respectively.

Elemental analyses were performed by Analytical Services, Department of Chemistry, University of Calgary, Calgary, Alberta, and by Canadian Microanalytical Service Ltd., Vancouver, British Columbia.

X-ray Crystallography. Crystals of $ClM[PhB(N^tBu)_2]$ (**1a**, M = As; **1b**, M = Sb; **1c**, M = Bi), $[PhB(N^tBu)_2]M\text{-}\mu\text{-}N(^t\text{Bu})B(Ph)N\text{-}(^t\text{Bu})M[PhB(N^tBu)_2]$ (**2b**, M = Sb; **2c**, M=Bi) and $LiM[PhB(N^t\text{-}$

(7) Manke, D. R.; Nocera, D. G. *Inorg. Chem.* **2003**, *42*, 4431.
(8) For a recent review, see: Fedorchuk, C.; Copsey, M. C.; Chivers, T. *Coord. Chem. Rev.* [Online early access] DOI: 10.1016/j.ccr.2006.06.010. Published Online: June 27, 2006.
(9) Chivers, T.; Fedorchuk, C.; Schatte, G.; Parvez. *Inorg. Chem.* **2003**, *42*, 2084.
(10) Manke, D. R.; Loh, Z-H.; Nocera, D. G. *Inorg. Chem.* **2004**, *43*, 3618.
(11) Manke, D. R.; Nocera, D. G. *Polyhedron* **2006**, *25*, 493.
(12) Paetzold, P.; Hahnfeld, D.; Englert, U.; Wojnowski, W.; Dreczewski, B.; Pawelec, Z.; Walz, L. *Chem. Ber.* **1992**, *125*, 1073.
(13) Habben, C. D.; Heine, A.; Sheldrick, G. M.; Stalke, D. *Z. Naturforsch.* **1992**, *47b*, 1367.
(14) Geschwentner, M.; Noltemeyer, M.; Elter, G.; Meller, A. *Z. Anorg. Allg. Chem.* **1994**, *620*, 1403.
(15) Luthin, W.; Stratman, J.-G.; Elter, G.; Meller, A.; Heine, A.; Gornitzka, H. *Z. Anorg. Allg. Chem.* **1995**, *621*, 1995.
(16) Albrecht, T.; Elter, G.; Noltemeyer, M.; Meller, A. *Z. Anorg. Allg. Chem.* **1998**, *624*, 1514.
(17) Habben, C. D.; Heine, A.; Sheldrick, G. M.; Stalke, D.; Bühl, M.; von Ragué Schleyer, P. *Chem. Ber.* **1991**, *124*, 47.
(18) Habben, C. D.; Herbst-Irmer, R.; Noltemeyer, M. *Z. Naturforsch.* **1991**, *46b*, 625.
(19) Chivers, T.; Gao, X.; Parvez. *Angew. Chem., Int. Ed. Engl.* **1995**, *34*, 2549.
(20) Gudat, D.; Niecke, E.; Nieger, M.; Paetzold, P. *Chem. Ber.* **1988**, *121*, 565.
(21) Chivers, T.; Fedorchuk, C.; Schatte, G.; Brask, J. K. *Can. J. Chem.* **2002**, *80*, 821.

Table 1. Crystallographic Data for ClM[PhB(N^{t}Bu)$_2$] (**1a**, M = As; **1b**, M = Sb; **1c**, M = Bi), [PhB(N^{t}Bu)$_2$]M-μ-N(^{t}Bu)B(Ph)N(^{t}Bu)-M[PhB(N^{t}Bu)$_2$] (**2b**, M = Sb; **2c**, M = Bi), and LiM[PhB(N^{t}Bu)$_2$]$_2$ (**3a**, **3a**·OEt$_2$, M = As; **3b**, M = Sb; **3c**·OEt$_2$, M = Bi)[a]

	1a	**1b**	**1c**	**2b**	**2c**	**3a**	**3a**·OEt$_2$	**3b**	**3c**·OEt$_2$
empirical formula	$C_{14}H_{23}AsClN_2$	$C_{14}H_{23}BClN_2Sb$	$C_{14}H_{23}BBiClN_2$	$C_{42}H_{69}B_3N_6Sb_2$	$C_{42}H_{69}B_3Bi_2N_6$	$C_{28}H_{46}AsB_2LiN_4$	$C_{32}H_{56}AsB_2LiN_4O$	$C_{28}H_{46}B_2LiN_4Sb$	$C_{32}H_{56}B_2BiLiN_4O$
fw	340.52	387.35	474.58	933.96	1108.42	542.17	616.29	589.00	750.35
cryst syst	triclinic	triclinic	monoclinic	monoclinic	monoclinic	monoclinic	triclinic	monoclinic	monoclinic
space group	$P\bar{1}$	$P\bar{1}$	C2/*m*	C2/*c*	C2/*c*	C2/*c*	$P\bar{1}$	C2/*c*	$P2_1/c$
a (Å)	6.000(1)	9.140(2)	33.164(7)	20.053(4)	20.239(4)	25.990(5)	10.050(2)	25.878(5)	12.067(2)
b (Å)	10.653(2)	11.328(2)	9.341(2)	17.3372(4)	17.659(4)	8.672(2)	10.148(2)	8.712(2)	20.280(4)
c (Å)	13.411(3)	17.090(3)	5.540(1)	15.402(3)	15.205(3)	18.403(4)	18.845(4)	18.521(4)	14.304(3)
α (deg)	94.16(3)	91.53(3)	90.00	90.00	90.00	90.00	82.92(3)	90.00	90.00
β (deg)	96.76(3)	102.55(3)	92.13	119.15(3)	120.23(3)	134.22(3)	84.57(3)	133.85(3)	94.44(3)
γ (deg)	99.49(3)	90.16(3)	90.00	90.00	90.00	90.00	66.12(3)	90.00	90.00
V (Å^3)	835.9(3)	1726.4(6)	1714.8(6)	4686(2)	4695(2)	2973(2)	1741.9(7)	3011(2)	3490(1)
Z	2	4	4	4	4	4	2	4	4
ρ_{calcd} (g/cm^3)	1.353	1.490	1.838	1.324	1.568	1.212	1.175	1.299	1.428
μ(Mo Kα) (mm^{-1})	2.182	1.742	10.427	1.187	7.519	1.166	1.005	0.939	5.081
Θ range (deg)	3.67−25.03	2.96−25.03	2.86−25.01	3.53−25.03	3.50−25.03	3.39−25.02	3.47−25.03	3.41−25.03	3.36−25.03
reflns collected	5606	8757	2898	15 577	12 211	9494	11 591	8355	11 814
unique reflns	2944	6018	1602	4123	4113	2620	6097	2650	6134
R_{int}	0.0257	0.0247	0.0423	0.0320	0.0499	0.0371	0.0272	0.0979	0.0303
reflns [$I>2\sigma(I)$]	2598	5429	1404	3485	3132	2385	5598	1758	5421
R_1 [$I > 2\sigma(I)$] [b]	0.0555	0.0333	0.0441	0.0268	0.0312	0.0533	0.0287	0.0662	0.0274
wR2 (all data)[c]	0.1544	0.0862	0.1010	0.0650	0.0637	0.1342	0.0724	0.1419	0.0737
GOF on F^2	1.140	1.139	1.215	1.071	1.015	1.157	1.025	1.061	1.048

[a] λ(Mo Kα) = 0.71073 Å, T = −100 °C. [b] $R_1 = \sum||F_o| - |F_c||/\sum|F_o|$. [c] wR2 = $[\sum w(F_o^2 - F_c^2)^2/\sum wF_o^4]^{1/2}$.

Bu)$_2$]$_2$ (**3a**, **3a**·OEt$_2$, M═As; **3b**, M═Sb; **3c**·OEt$_2$, M = Bi) were coated with Paratone 8277 oil and mounted on a glass fiber. Diffraction data were collected on a Nonius KappaCCD diffractometer using monochromated Mo Kα radiation (λ = 0.71073 Å) at −100 °C. The data sets were corrected for Lorentz and polarization effects, and empirical absorption correction was applied to the net intensities. The structures were solved by direct methods using SHELXS-97[22] and refined using SHELXL-97.[23] After the full-matrix least-squares refinement of the non-hydrogen atoms with anisotropic thermal parameters, the hydrogen atoms were placed in calculated positions [C−H = 0.98 Å for C(C*H*$_3$)$_3$ and 0.95 Å for phenyl hydrogens]. The isotropic thermal parameters of the hydrogen atoms were fixed at 1.2 times that of the corresponding carbon for phenyl hydrogens and 1.5 times for C(C*H*$_3$)$_3$. In the final refinement, the hydrogen atoms were riding with the carbon atom to which they were bonded.

In the structures of **3a** and **3b**, the lithium and group 15 atom positions were disordered with the atoms statistically distributed over the two atomic sites. In both structures, the two atoms were not constrained to locate in the same position, but the anisotropic thermal parameters were restricted to be equal. The site occupation factors were fixed to be 50% in both cases. The structure of **1c** was also disordered, the second molecule being generated by symmetry over the bismuth and a nitrogen atom (50% site occupation factors). The scattering factors for the neutral atoms were those incorporated with the programs. Crystallographic data are summarized in Table 1.

Synthesis of ClAs[PhB(N^{t}Bu)$_2$] (1a). A solution of $AsCl_3$ (0.181 g, 1.00 mmol) in diethyl ether (15 mL) was cooled to −80 °C, and a solution of Li$_2$[PhB(N^{t}Bu)$_2$] (0.244 g, 1.00 mmol) in diethyl ether (15 mL) was added via cannula. The reaction mixture was stirred for 1/2 h at −80 °C and ∼4 h at room temperature. LiCl was removed by filtration, and the solvent was evaporated under vacuum to give **1a** as an analytically pure, white solid (0.296 g, 87%). Anal. Calcd for $C_{14}H_{23}AsBClN_2$: C, 49.38; H, 6.81; N, 8.23. Found: C, 48.77; H, 6.92; N, 7.92. ^{1}H NMR (toluene-d_8, 23 °C): δ 7.08−7.36 [m, 5H, C$_6$*H*$_5$], 1.08 [s, 18H, C(C*H*$_3$)$_3$]. ^{13}C{^{1}H} NMR: δ 127.9−131.2 [C$_6$H$_5$], 52.6 [s, *C*(CH$_3$)$_3$], 32.8 [s, C(*C*H$_3$)$_3$]. ^{11}B NMR: δ 37.3. Colorless crystals of **1a** were obtained from *n*-hexane after 4 days at 5 °C.

Synthesis of ClSb[PhB(N^{t}Bu)$_2$] (1b). Compound **1b** was obtained as a pale yellow powder (0.180 g, 78%) from the reaction of Li$_2$[PhB(N^{t}Bu)$_2$] (0.147 g, 0.60 mmol) with $SbCl_3$ (0.137 g, 0.60 mmol) in diethyl ether via the method described for **1a**. Anal. Calcd for $C_{14}H_{23}SbBClN_2$: C, 43.41; H, 5.98; N, 7.23. Found: C, 42.82; H, 6.50; N, 6.86. ^{1}H NMR (toluene-d_8, 23 °C): δ 7.10−7.43 [m, 5H, C$_6$*H*$_5$], 1.00 [s, 18H, C(C*H*$_3$)$_3$]. ^{13}C{^{1}H} NMR: δ 127.7−131.2 [C$_6$H$_5$], 51.7 [*C*(CH$_3$)$_3$], 34.2 [C(*C*H$_3$)$_3$]. ^{11}B NMR: δ 39.4. Pale yellow crystals of **1b** were obtained from *n*-hexane in 24 h at −20 °C.

Synthesis of ClBi[PhB(N^{t}Bu)$_2$] (1c). Compound **1c** was obtained as a red powder (0.188 g, 79%) from the reaction of Li$_2$[PhB(N^{t}Bu)$_2$] (0.122 g, 0.50 mmol) with $BiCl_3$ (0.158 g, 0.50 mmol) in diethyl ether via the method described for **1a**. Anal. Calcd for $C_{14}H_{23}BiBClN_2$: C, 35.43; H, 4.88; N, 5.90. Found: C, 36.10; H, 5.22; N, 5.71. ^{1}H NMR (toluene-d_8, 23 °C): δ 7.15−7.59 [m, 5H, C$_6$*H*$_5$], 0.95 [s, 18H, C(C*H*$_3$)$_3$]. ^{13}C{^{1}H} NMR: δ 127.4−131.2 [C$_6$H$_5$], 50.7 [*C*(CH$_3$)$_3$], 36.2 [C(*C*H$_3$)$_3$]. ^{11}B NMR: δ 38.5. Orange crystals of **1c** were grown from *n*-hexane in 3 h at −20 °C.

Synthesis of [PhB(N^{t}Bu)$_2$]Sb-μ-N(^{t}Bu)B(Ph)N(^{t}Bu)-Sb[PhB(N^{t}Bu)$_2$] (2b). A solution of Li$_2$[PhB(N^{t}Bu)$_2$] (0.220 g, 0.90 mmol) in 15 mL of diethyl ether was added to a solution of $SbCl_3$ (0.137 g, 0.60 mmol) in 15 mL of Et_2O at −80 °C. The reaction mixture was stirred for 1/2 h at −80 °C and 4 h at 23 °C. LiCl was removed by filtration, and the solvent was evaporated under vacuum to give **2b** as an amorphous, pale yellow powder (0.203 g, 73%). Anal. Calcd for $C_{42}H_{69}B_3N_6Sb_2$: C, 54.01; H, 7.45; N, 9.00. Found: C, 53.61; H, 7.53; N, 8.62. ^{1}H NMR (toluene-d_8, 23 °C): δ 7.17−7.92 [m, 15H, C$_6$*H*$_5$], 1.65 [s, 18H, bridging C(C*H*$_3$)$_3$], 1.33 [s, 18H, chelating C(C*H*$_3$)$_3$], 1.32 [s, 18H, chelating C(C*H*$_3$)$_3$]. ^{13}C{^{1}H} NMR: δ 127.3−134.9 [C$_6$H$_5$], 61.4 [bridging *C*(CH$_3$)$_3$], 52.4 [chelating *C*(CH$_3$)$_3$], 52.3 [chelating *C*(CH$_3$)$_3$], 36.3 [C(*C*H$_3$)$_3$], 35.5

(22) Sheldrick, G. M. *SHELXS-97, Program for Crystal Structure Determination*; University of Göttingen: Göttingen, Germany, 1997.
(23) Sheldrick, G. M. *SHELXL-97, Program for Crystal Structure Refinement*; University of Göttingen: Göttingen, Germany, 1997.

$[C(CH_3)_3]$, 35.4 $[C(CH_3)_3]$. ^{11}B NMR: δ 39.4 (br). X-ray quality crystals of **2b** were obtained from a concentrated solution of toluene or diethyl ether in 24 h at 23 °C.

Synthesis of [PhB(N^{t}Bu)$_2$]Bi-μ-N(^{t}Bu)B(Ph)N(^{t}Bu)-Bi[PhB(N^{t}Bu)$_2$] (2c). Compound **2c** was obtained as an orange powder (0.151 g, 68%) from the reaction of $Li_2[PhB(N^tBu)_2]$ (0.146 g, 0.60 mmol) with $BiCl_3$ (0.126 g, 0.40 mmol) in Et_2O via the method described for **2b**. Anal. Calcd for $C_{42}H_{69}B_3N_6Bi_2$: C, 45.51; H, 6.27; N, 7.58. Found: C, 45.30; H, 6.08; N, 7.39. ^1H NMR (toluene-d_8, 23 °C): δ 7.12−7.89 [m, 15H, C_6H_5], 1.64 [s, 18H, bridging $C(CH_3)_3$], 1.26 [s, 18H, chelating $C(CH_3)_3$], 1.21 [s, 18H, chelating $C(CH_3)_3$]. $^{13}C\{^1H\}$ NMR: δ 127.4−134.9 [C_6H_5], 61.5 [bridging $C(CH_3)_3$], 52.1 [chelating $C(CH_3)_3$], 51.9 [chelating $C(CH_3)_3$], 37.6 $[C(CH_3)_3]$, 37.4 $[C(CH_3)_3]$, 37.1 $[C(CH_3)_3]$. ^{11}B NMR: δ 34.3 (br). X-ray quality crystals of **2c** were obtained from *n*-hexane in 5 days at −20 °C.

Synthesis of LiAs[PhB(N^{t}Bu)$_2$]$_2$ (3a). A solution of $Li_2[PhB(N^tBu)_2]$ (0.244 g, 1.00 mmol) in 15 mL of Et_2O was added to a solution of $AsCl_3$ (0.091 g, 0.50 mmol) in 15 mL of Et_2O at −80 °C. The reaction mixture was stirred for 1/2 h at −80 °C and 16 h at 23 °C. LiCl was removed by filtration, and the solvent was concentrated to ∼2 mL. Crystallization from diethyl ether afforded **3a** after 5 days at 5 °C (0.151 g, 56%). Although a few crystals of **3a**·OEt_2 were also obtained, the NMR data indicates that unsolvated **3a** is the main product. Anal. Calcd for $C_{28}H_{46}AsB_2LiN_4$: C, 62.03; H, 8.55; N, 10.33. Found: C, 62.01; H, 8.41; N, 10.02. ^1H NMR (toluene-d_8, 23 °C): δ 7.13−7.68 [m, 10H, C_6H_5], 1.39 [s, 9H, $C(CH_3)_3$], 1.30 [s, 18H, $C(CH_3)_3$], 1.22 [s, 9H, $C(CH_3)_3$]. $^{13}C\{^1H\}$ NMR: δ 126.9−134.0 [s, C_6H_5], 56.8 [s, $C(CH_3)_3$], 53.1 [s, $C(CH_3)_3$], 50.1 [s, $C(CH_3)_3$], 35.3 [s, $C(CH_3)_3$], 34.3 [s, $C(CH_3)_3$], 33.6 [s, $C(CH_3)_3$]. ^{11}B NMR: δ 34.1. ^7Li NMR: δ 1.27.

Synthesis of LiSb[PhB(N^{t}Bu)$_2$]$_2$ (3b). A solution of $Li_2[PhB(N^tBu)_2]$ (0.195 g, 0.80 mmol) in 15 mL of THF was added to a solution of $SbCl_3$ (0.091 g, 0.40 mmol) in 15 mL of THF at −80 °C. The reaction mixture was stirred for 1/2 h at −80 °C and then heated to 65 °C for 6 h. Solvent was removed in vacuo, and the pale yellow residue was dissolved in∼20 mL of Et_2O. LiCl was removed by filtration, and the solvent was concentrated to ∼2 mL. Crystallization from Et_2O afforded **3b** as pale yellow crystalline material after 2 days at 5 °C (0.043 g, 18%). ^1H NMR (toluene-d_8, 23 °C): δ 7.10−7.61 [m, 10H, C_6H_5], 1.21 [s, 36H, $C(CH_3)_3$]. $^{13}C\{^1H\}$ NMR: δ 127.1−134.1 [C_6H_5], 50.2 [$C(CH_3)_3$], 34.8 $[C(CH_3)_3]$. ^{11}B NMR: δ 34.9. ^7Li NMR: δ 1.05. The purity of **3b** was indicated by the NMR data; however, several attempts to obtain accurate CHN data were unsuccessful.

Synthesis of LiBi[PhB(N^{t}Bu)$_2$]$_2$·OEt$_2$ (3c·OEt$_2$). A solution of $Li_2[PhB(N^tBu)_2]$ (0.195 g, 0.80 mmol) in 15 mL of Et_2O was added to a suspension of $BiCl_3$ (0.126 g, 0.40 mmol) in 15 mL of Et_2O at −80 °C. The reaction mixture was allowed to reach room temperature in 1/2 h and was then heated to 35 °C for 16 h. LiCl was removed by filtration, and the solvent was evaporated in vacuo. The precipitate was washed with cold *n*-hexane (0 °C) giving **3c**·OEt_2 as a yellow powder (0.195 g, 65%). ^1H NMR (toluene-d_8, 23 °C): δ 7.15−7.50 [m, 10H, C_6H_5], 3.46 [q, 4H, $(CH_3CH_2)_2O$], 1.31 [s, 36H, $C(CH_3)_3$], 1.108 [t, 6H, $(CH_3CH_2)_2O$]. $^{13}C\{^1H\}$ NMR: δ 125.9−134.9 [C_6H_5], 65.1 [$(CH_3CH_2)_2O$], 53.8 [$C(CH_3)_3$] 36.8 $[C(CH_3)_3]$, 14.7 $[(CH_3CH_2)_2O]$. ^{11}B NMR: δ 35.1. ^7Li NMR: 0.19. Recrystallization from Et_2O gave yellow X-ray quality crystals of **3c**·OEt_2 after 6 h at 23 °C. Accurate CHN data could not be obtained for **3c·OEt$_2$** because of partial loss of OEt_2 during manipulation of the sample.

Results and Discussion

Synthesis, NMR Spectra, and Crystal Structures of ClM[PhB(N^{t}Bu)$_2$] (1a, M = As; 1b, M = Sb; 1c, M = Bi). Analytically pure mono-boraamidinates $ClM[PhB(N^tBu)_2]$ (**1a**−**c**) are readily obtained in excellent yields by the reaction of MCl_3 with $Li_2[PhB(N^tBu)_2]$ in a 1:1 molar ratio in diethyl ether (eq 1). The compounds **1a**−**c** were characterized by multinuclear NMR spectroscopy in solution and by X-ray crystallography in the solid state.

$$MCl_3 + Li_2[PhB(N^tBu)_2] \rightarrow ClM[PhB(N^tBu)_2] + 2\ LiCl$$
$$M = As\ (\mathbf{1a}),\ Sb\ (\mathbf{1b}),\ Bi\ (\mathbf{1c}) \qquad (1)$$

The NMR spectra of **1a**−**c** in toluene-d_8 are consistent with the replacement of two Cl atoms in MCl_3 by the bam ligand. The ^1H NMR spectrum is composed of a singlet attributed to the $C(CH_3)_3$ hydrogens and a multiplet for the phenyl hydrogens. The $^{13}C\{^1H\}$ NMR spectrum shows singlets for the $C(CH_3)_3$ and $C(CH_3)_3$ carbon atoms, as well as the characteristic phenyl resonances. The ^1H NMR resonance of the $C(CH_3)_3$ hydrogens shifts to lower frequency, and the multiplet observed for the phenyl group exhibits a slight displacement to higher frequency on going from **1a** to **1c**. Concomitantly, the ^{13}C NMR resonance for the $C(CH_3)_3$ carbons shifts to higher frequency and the α-carbon of the $C(CH_3)_3$ groups exhibits a singlet at lower frequency along the series **1a**−**c**. The changes in the ^{13}C chemical shifts of the phenyl carbon signals are rather small. The ^{11}B NMR spectra of **1a**−**c** display a broad singlet in the range of 37.3−39.4 ppm consistent with the presence of three-coordinate boron centers.

The crystal structures of **1a**−**c** are depicted in Figure 1, and the pertinent bond parameters are presented in Table 2. The observed disorder in structure **1c** results in high standard deviations in the bond parameters. The molecular units of **1a**−**c** (Figure 1a) are isostructural with the previously reported group 15 mono-bam, $BrP[PhB(N^tBu)_2]$ (**1d**),[21] and exhibit bonding mode **A** (Scheme 1). The crystal packing, however, is distinct because of the increasing strength of the intermolecular M···Cl (M = As, Sb, Bi) close contacts for the heavier metal centers. Whereas the phosphorus- and arsenic-containing compounds, **1d**[21] and **1a**, adopt a packing arrangement without significant intermolecular close contacts in the crystal lattice, the antimony complex **1b** shows weak Sb···Cl contacts between the neighboring molecules giving rise to infinite chains of the mono-boraamidinates (Figure 1b). The bismuth analogue **1c** exhibits similar infinite chains. The Bi···Cl close contacts along the chain, however, are significantly stronger than in **1b** [3.495(1) Å in **1b** vs 3.134(5) Å in **1c**]. In addition, **1c** displays a second, significantly weaker, Bi···Cl contact [3.784(6) Å], thus inducing infinite chains of *dimeric* units in the solid state (Figure 1c).

The M−Cl bond length increases by ∼0.2 Å from **1a** to **1b** and from **1b** to **1c** corresponding to an increase in the size of the group 15 center. The calculated M−Cl bond order[24] is somewhat lower in **1c** than that in **1a** and **1b** (0.54 for **1c** and ∼0.84 for **1a** and **1b**). This difference is attributed

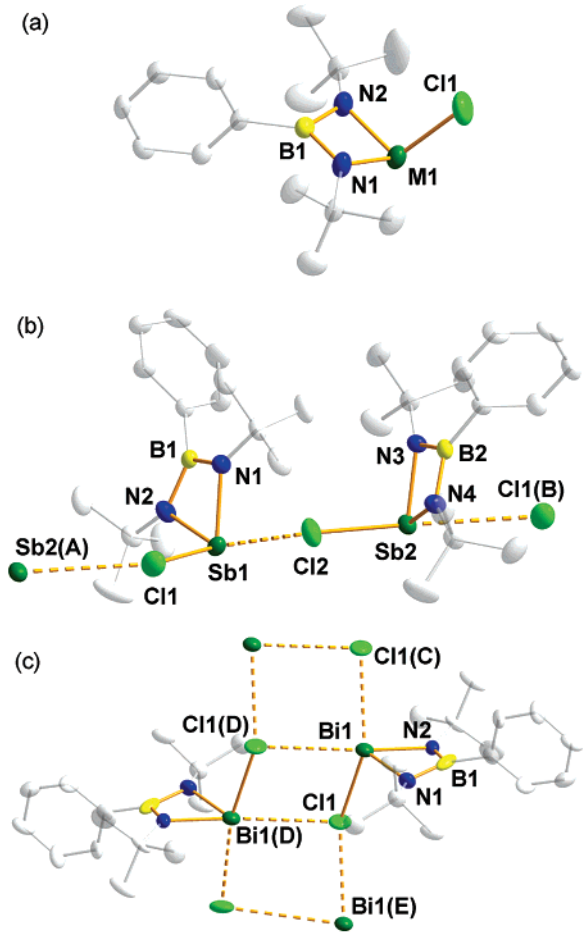

Figure 1. Molecular structures of ClM[PhB(N^{t}Bu)$_2$] with the atomic numbering schemes: (a) the monomeric unit of **1a** (M = As), (b) Sb···Cl close contacts in the infinite chains of **1b** (M = Sb), and (c) Bi···Cl close contacts in the dimeric infinite chains of **1c** (M = Bi). Hydrogen atoms have been omitted for clarity. Symmetry operations: (A) $x, y + 1, z$. (B) $x, y - 1, z$. (C) $x, y, z - 1$. (D) $1 - x, y, 2 - z$. (E) $x, y, z + 1$.

Table 2. Selected Bond Lengths (Å) and Angles (deg) in XM[PhB(N^{t}Bu)$_2$] [X = Br, M = P (**1d**);[21] X = Cl, M = As (**1a**), Sb (**1b**), Bi (**1c**)][a]

	1d[b]	**1a**[c]	**1b**[d]	**1c**[e]
M1−N1	1.688(3)	1.846(5)	2.024(3)	2.11(2)
M1−N2	1.688(3)	1.839(5)	2.031(3)	2.15(1)
M1−Cl1	2.305(1)[f]	2.229(2)	2.427(1)	2.638(5)
	[0.81]	[0.85]	[0.83]	[0.54]
N1−B1	1.440(4)	1.448(8)	1.443(5)	1.46(4)
N2−B1	1.440(4)	1.441(8)	1.443(5)	1.46(3)
M···Cl1′			3.495(1)[g]	3.134(5)[h]
M···Cl1″				3.784(6)[i]
N1−M1−N2	80.1(1)	74.5(2)	69.0(1)	66.0(2)
N1−M1−Cl1	103.7(1)[f]	102.5(2)	100.64(9)	96.9(4)
N2−M1−Cl1	103.7(1)[f]	103.2(2)	99.83(9)	100.3(3)
M1−N1−B1	90.4(2)	90.9(4)	91.3(2)	93(1)
M1−N2−B1	90.4(2)	91.4(3)	91.6(2)	92(1)
N1−B1−N2	97.9(3)	101.0(5)	105.5(3)	105(2)

[a] Calculated bond orders in square brackets.[24] [b] M = P. [c] M = As. [d] M = Sb (bond parameters of the second independent molecule are within experimental error). [e] M = Bi. [f] Cl = Br. [g] Symmetry operation: $x, y - 1, z$. [h] Symmetry operation: $x, y, z - 1$. [i] Symmetry operation: $1 - x, y, 2 - z$.

to the strong intermolecular Bi···Cl close contacts observed for **1c**. The B−N bond lengths of the bam unit in **1a**−**d** are all equal within the experimental error, while the M−N bond

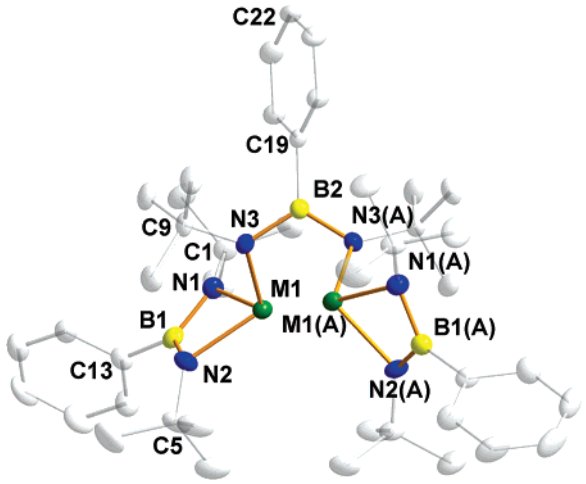

Figure 2. Molecular structure of [PhB(N^{t}Bu)$_2$]M-μ-N(^{t}Bu)B(Ph)N(^{t}Bu)-M[PhB(N^{t}Bu)$_2$] (**2b**, M = Sb) with the atomic numbering scheme. The bismuth complex **2c** (M = Bi) is isostructural with **2b**. Hydrogen atoms have been omitted for clarity. Symmetry operation: (A) $1 - x, y, 1.5 - z$.

lengths show the expected elongation with increasing size of the group 15 atom. The endocyclic bond angles at the group 15 center decrease significantly along the series **1d**−**1a**−**1b**−**1c,** while there is a corresponding increase in the endocyclic bond angle at boron. The stereochemical influence of the lone pair is readily apparent from the trend in the sum of the bond angles at the group 15 center [287.5° (**1d**), 280.2° (**1a**), 269.5° (**1b**), and 263.2° (**1c**)], reflecting the increasing s character as one descends the group.

Synthesis, Crystal Structures, and NMR Spectra of [PhB(N^{t}Bu)$_2$]M-μ-N(^{t}Bu)B(Ph)N(^{t}Bu)-M[PhB(N^{t}Bu)$_2$] (2b, M = Sb; 2c, M = Bi). The novel 2:3 boraamidinate complexes **2b** and **2c** are obtained in good yields by the reaction of MCl_3 with Li_2[PhB(N^{t}Bu)$_2$] (M=Sb, Bi) in a 1:1.5 molar ratio in diethyl ether (eq 2). Attempts to produce the arsenic analog **2a** with this method or the reaction between **1a** and Li_2[PhB(N^{t}Bu)$_2$] in Et_2O resulted in a mixture of the mono- and bis-boraamidinates, **1a** and **3a**, as revealed by a combination of NMR spectroscopy and X-ray crystallography. A small amount of unidentified byproducts was also evident in the NMR spectra.

$$2MCl_3 + 3Li_2[PhB(N^tBu)_2] \rightarrow M_2[PhB(N^tBu)_2]_3 + 6LiCl$$
$$M = Sb\ (\mathbf{2b}),\ Bi\ (\mathbf{2c}) \qquad (2)$$

The molecular structures of **2b** and **2c** with the atomic numbering scheme are depicted in Figure 2, and selected bond parameters are summarized in Table 3. The isostructural 2:3 boraamidinate complexes **2b** and **2c** are composed of two metal centers N,N′-chelated by a bam ligand; the two $[M(bam)]^+$ units are bridged by the third $[bam]^{2-}$ ligand, thus combining the bonding modes **A** and **F** (Scheme 1). The compounds show C_2 symmetry through the boron atom B2 and the phenyl carbon atoms C19 and C22 of the bridging

(24) The bond orders were calculated by the Pauling equation $N = 10^{(D-R)/0.71}$,[25] where R is the observed bond length (Å). The single bond length D is estimated from the sums of appropriate covalent radii (Å):[25] P−Br = 2.24, As−Cl = 2.18, Sb−Cl = 2.37, Bi−Cl = 2.45.

Table 3. Selected Bond Lengths (Å) and Angles (deg) in [PhB(N^{t}Bu)$_2$]M-μ-N(^{t}Bu)B(Ph)N(^{t}Bu)-M[PhB(N^{t}Bu)$_2$] (M = Sb, Bi)

	2b[a]	**2c**[b]		**2b**[a]	**2c**[b]
M1−N1	2.067(2)	2.162(5)	B1−N1	1.430(4)	1.439(8)
M1−N2	2.077(2)	2.195(4)	B1−N2	1.439(4)	1.450(8)
M1−N3	2.082(2)	2.213(3)	B2−N3	1.463(4)	1.457(6)
N1−M1−N2	67.3(1)	64.7(2)	N3−B2−C19	121.2(2)	122.6(3)
N1−M1−N3	106.12(9)	106.1(2)	M1−N3−B2	109.1(2)	106.5(3)
N2−M1−N3	109.22(9)	108.0(2)	M1−N3−C9	125.3(2)	124.5(3)
N1−B1−N2	106.3(3)	107.7(5)	B2−N3−C9	124.6(2)	126.5(4)
N3−B2−N3(A)[c]	117.6(3)	114.8(7)	M1−N3−B2−N3(A)[c]	50.5(2)	50.6(3)

[a] M = Sb. [b] M = Bi. [c] Symmetry operation: $-x, y, 1.5 - z$.

[bam]$^{2-}$ ligand. The nitrogen and boron atoms of the bridging [bam]$^{2-}$ ligand adopt trigonal planar geometry (sum of the bond angles on N(3) and B(2) are 359.0 and 360.0° in **2b** and 357.5 and 360.0° in **2c**, respectively). The two [M(bam)]$^+$ units are arranged in a cis fashion with respect to the bridging [bam]$^{2-}$ ligand. The nearly planar MNBN rings are tilted in a manner that reflects the influence of the lone pair on the metal. Despite the size difference between antimony and bismuth, and the resulting differences in the M−N bond lengths, the torsion angles M1−N3−B2−N3(A) are equal at ∼50.5°. In addition to controlling the structural features of **2b** and **2c**, we also tentatively attribute the lack of formation of the arsenic analogue **2a** to the steric requirements of the lone pair, that is, the shorter As−N bonds would lead to untenable interference between the ^{t}Bu-groups of the chelating and bridging bam ligands under the influence of the lone pair on arsenic.

The three M−N and B−N bond lengths span the narrow ranges of 2.067(2)−2.082(2) and 1.430(4)−1.463(4) Å in **2b** and 2.162(5)−2.213(3) and 1.439(8)−1.457(6) Å in **2c**. For both compounds, the bond lengths increase in the order M1−N1 < M1−N2 < M1−N3 and B1−N1 < B1−N2 < B2−N3, that is, the longest bonds involve the bridging bam ligand. The average M−N bond lengths involving the chelating bam ligand in **2b** and **2c** are ∼0.05 Å longer than those in the mono-boraamidinates **1b** and **1c**, whereas the corresponding differences in the B−N bond lengths of the chelating boraamidinates are not significant. Expectedly, the N−B−N bond angle in the bridging bam ligand is significantly wider than that in the chelating ligand, by ∼10° in **2b** and 7° in **2c**. For both compounds, the N2−M1−N3 angle is somewhat wider than the N1−M1−N3 angle. The sum of the bond angles at the pyramidal group 15 center are 282.6° (**2b**) and 278.8° (**2c**).

The ^{1}H NMR spectra of **2b** and **2c** in toluene-d_8 are composed of three singlets in a 1:1:1 intensity ratio attributed to the C(CH$_3$)$_3$ hydrogens and a multiplet for the phenyl hydrogens. Consistently, the ^{13}C{^{1}H} NMR spectra display three singlets for both the *C*(CH$_3$)$_3$ and C(*C*H$_3$)$_3$ carbons, as well as the expected resonances for phenyl carbons. The three equally intense singlets observed for the ^{t}Bu groups are assigned to the units bonded to N(1), N(2), and N(3), respectively. The influence of the lone pair on the group 15 atom is evident from the NMR data of **2b** and **2c**, which are consistent with a stereochemically rigid structure in solution involving nonfluxional [M(bam)]$^+$ units bridged by the third [bam]$^{2-}$ ligand. The ^{11}B NMR spectra for **2b** and **2c** show only one very broad resonance, presumably as a result of overlap of broad signals with similar chemical shifts for the different three-coordinate boron environments, B1/B1(A) and B2.

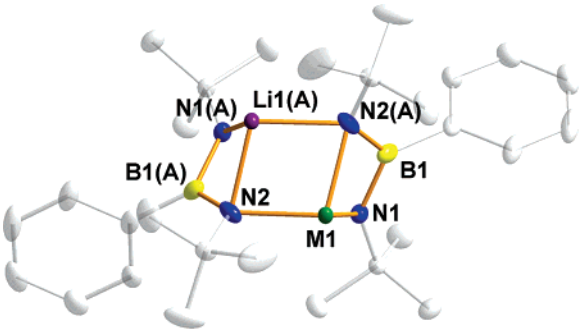

Figure 3. Molecular structure of LiM[PhB(N^{t}Bu)$_2$]$_2$ (**3a**, M = As) with the atomic numbering scheme. Hydrogen atoms have been omitted for clarity. The antimony complex **3b** (M = Sb) is isostructural with **3a**. Symmetry operation: (A) $-x, y, 0.5 - z$.

Synthesis of LiM[PhB(N^{t}Bu)$_2$]$_2$ (3a, M = As; 3b, M = Sb; 3c, M = Bi). The reaction of MCl$_3$ (M = As, Bi) with Li$_2$[PhB(N^{t}Bu)$_2$] in diethyl ether and treatment of SbCl$_3$ with Li$_2$[PhB(N^{t}Bu)$_2$] in THF in a 1:2 molar ratio produce the bis-boraamidinates LiM[PhB(N^{t}Bu)$_2$]$_2$ (**3a**−**c**) (eq 3).

$$MCl_3 + 2Li_2[PhB(N^tBu)_2] \rightarrow LiM[PhB(N^tBu)_2] + 3LiCl$$
$$[M = As\ (\mathbf{3a}),\ Sb\ (\mathbf{3b}),\ Bi\ (\mathbf{3c})] \qquad (3)$$

After recrystallization, both unsolvated (**3a**) and solvated (**3a**·OEt$_2$) complexes were obtained for arsenic, while only the unsolvated complex was isolated for antimony (**3b**) and the solvated complex (**3c**·OEt$_2$) crystallized for bismuth. Although the arsenic-containing bis-bam **3a** is readily obtained by conducting the reaction at room temperature, the formation of the bismuth analogue, **3c**·OEt$_2$, requires elevated temperature for completion. The room-temperature reaction resulted in a mixture of the bis-bam **3c**·OEt$_2$, the 2:3 complex **2c**, and unreacted Li$_2$[PhB(N^{t}Bu)$_2$] as revealed by NMR spectroscopy. The antimony complex **3b** was obtained only in moderate yields after a reaction in boiling THF, while the room-temperature reactions in various solvents and the reaction in boiling Et$_2$O produced mainly the 2:3 complex **2b**.

Crystal Structures of LiM[PhB(N^{t}Bu)$_2$]$_2$ (3a, M = As; 3b, M = Sb) and Li(OEt$_2$)M[PhB(N^{t}Bu)$_2$]$_2$ (3a·OEt$_2$, M = As; 3c·OEt$_2$, M = Bi). The disordered structures of the unsolvated bis-boraamidinates **3a** and **3b** exhibit a ladder arrangement (bonding mode **B** in Scheme 1), which is analogous to that previously observed for the tin(II) and lead(II) complexes, {Sn[MeB(NSiMe$_3$)(NSiMe$_3$)]}$_2$ and {Pb[PhB(N^{t}Bu)(N^{t}Bu)]}$_2$.[1,2] The molecular structures of **3a** and **3b** are composed of two four-membered rings, BN$_2$Li and BN$_2$M (M = As, Sb), connected by Li−N and M−N bonds thus forming tricyclic compounds with three- and four-coordinate nitrogens (Figure 3). Selected bond parameters for **3a** and **3b** are compared to those of **3a**·OEt$_2$ and **3c**·OEt$_2$ in Table 4. The B−N bond lengths in **3a** and **3b** show

Table 4. Selected Bond Lengths (Å) and Angles (deg) in $LiM[PhB(N^tBu)_2]_2$ (M = As, Sb, Bi)

	3a[a]	**3b**[b]		**3a**[a]	**3b**[b]
M1−N1	1.789(3)	1.943(5)	Li1(A)[c]−N1(A)[c]	2.07(2)	1.64(4)
M1−N2	1.967(3)	2.145(5)	Li1[c]−N2(A)[c]	2.04(3)	2.28(4)
M1−N2(A)[c]	1.972(3)	2.198(5)	B1−N1	1.408(4)	1.407(8)
Li1(A)[c]−N2	1.95(3)	2.30(5)	B1−N2(A)[c]	1.461(5)	1.455(8)
N1−M1−N2	108.0(1)	104.2(2)	M1−N2(A)[c]−B1	79.2(1)	80.5(3)
N1−M1−N2(A)[c]	76.7(1)	69.1(2)	N1−B1−N2(A)[c]	109.2(3)	111.0(5)
N2−M1−N2(A)[c]	101.3(1)	98.5(2)	N1(A)[c]−B1(A)[c]−N2	109.0(3)	110.5(5)
M1−N1−B1	87.3(2)	91.4(4)	B1(A)[c]−N2−M1	126.4(2)	126.8(4)

	3a·OEt_2[a]	**3c**·OEt_2[d]		**3a**·OEt_2[a]	**3c**·OEt_2[d]
M1−N1	1.962(2)	2.274(3)	B2−N3	1.527(2)	1.456(5)
M1−N2	1.876(2)	2.283(3)	B2−N4	1.371(3)	1.418(5)
M1−N3	1.845(2)	2.239(3)	Li1−N1	2.092(3)	2.126(8)
M1−N4	3.327(2)	2.444(3)	Li1−N3	2.853(3)	2.128(7)
B1−N1	1.481(2)	1.485(5)	Li1−N4	1.902(3)	2.360(8)
B1−N2	1.412(3)	1.398(5)	Li1···O1	2.012(3)	1.922(7)
N1−M1−N2	72.45(6)	63.2(1)	N2−M1−N4	73.18(6)	149.6(1)
N1−M1−N3	109.38(7)	91.2(1)	N3−M1−N4	46.91(5)	59.6(1)
N1−M1−N4	72.37(5)	91.6(1)	N1−B1−N2	103.3(2)	111.7(3)
N2−M1−N3	111.05(7)	101.9(1)	N3−B2−N4	116.6(2)	108.3(5)

[a] M = As. [b] M = Sb. [c] Symmetry operation: $-x, y, 0.5 - z$. [d] M = Bi.

a slight inequality of ∼0.04 Å for both compounds. As expected, the M−N bonds to the three-coordinate nitrogen in **3a** and **3b** are ∼0.18 and 0.24 Å, respectively, shorter than those involving the four-coordinate nitrogens. The observed disorder in the structures results in inaccuracy in the lithium position preventing a detailed discussion of the bond parameters involving the lithium center.

The central four-membered MN_2Li (M = As, Sb) rings in **3a** and **3b** are nonplanar with mean torsion angles involving the four atoms of ∼12 and 5°, respectively. The three-coordinate boron and nitrogen atoms in **3a** and **3b** show a cis arrangement with respect to the central four-membered ring similar to that in $\{Sn[MeB(NSiMe_3)(NSiMe_3)]\}_2$,[1] but in contrast to the trans geometry observed in $\{Pb[PhB(N^t$-$Bu)(N^tBu)]\}_2$.[2] This divergence indicates that crystal packing, rather than the nature of the groups on nitrogen and boron, is the determining factor in the geometrical arrangement of these dimers.

The molecular structures of **3a**·OEt_2 and **3c**·OEt_2 are depicted in Figure 4, and the relevant bond parameters are listed in Table 4. The solvation of the lithium center by Et_2O in **3a** disrupts the ladder structure so that the transannular Li1···N3 and As1···N4 interactions are extremely weak (2.853(3) and 3.327(2) Å, respectively) resulting in essentially three-coordinate lithium and arsenic atoms in a bicyclic compound composed of a four-membered BN_2As and a six-membered BN_3AsLi ring (Figure 4a). For comparison, the spirocyclic group 13 complex $Li(OEt_2)Ga[PhB(\mu$-$N^tBu)_2]_2$ exhibits an almost perpendicular arrangement of the two four-membered GaNBN rings with four Ga−N and two Li−N bonds.[10] Similar M−N−Li interactions have been observed in homoleptic group 4 metal complexes of the type $M(bam)_3Li_2$ (M = Zr, Hf).[7] The lone pair on arsenic in **3a**·OEt_2, prevents the perpendicular arrangement of the bam ligands and therefore also contributes to the observed bonding arrangement. The lithium atom in **3a**·OEt_2 is strongly bonded

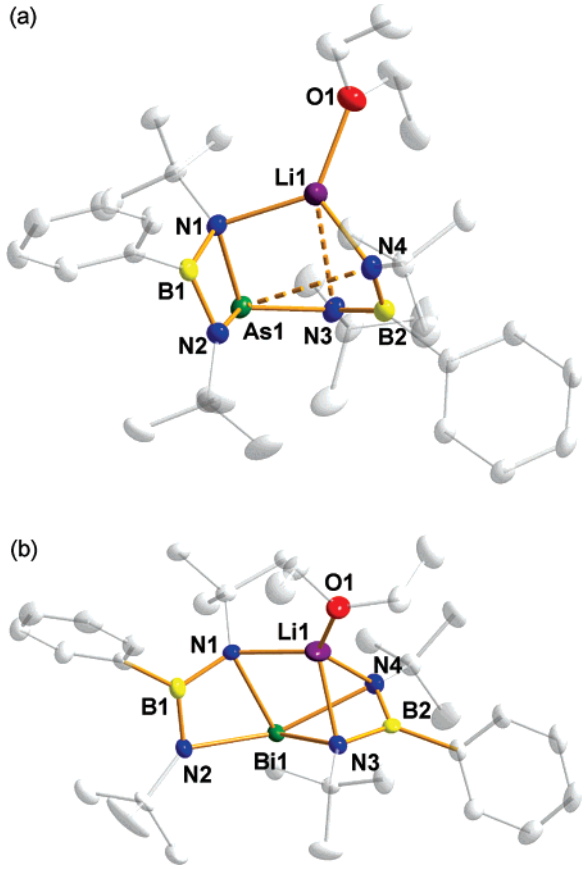

Figure 4. Crystal structures of (a) $Li(OEt_2)As[PhB(N^tBu)_2]_2$ (**3a**·OEt_2) and (b) $Li(OEt_2)Bi[PhB(N^tBu)_2]_2$ (**3c**·OEt_2) with the atomic numbering scheme. Hydrogen atoms have been omitted for clarity.

to one bam ligand [Li1−N4 = 1.902(3) Å], and it is also coordinated to the chelating bam ligand [Li1−N1 = 2.092-(3) Å]. The lack of a significant As1−N4 interaction results in a disparity of ∼0.16 Å in the B−N bond lengths of the bam ligand that bridges As1 and Li1. The B2−N3 distance of 1.371(3) Å is unusually short compared to the range of values reported for bam complexes.[8] A similar B−N bond length has been observed only in the gallium and indium complexes $\{[PhB(N^tBu)_2]GaCl\}_2$, $Li(THF)_4[PhB(N^tBu)_2]$-$GaCl_2$·$GaCl_3$, and $[PhB(N^tBu)_2]InCl_2$·$LiCl(THF)_2$ [B−N = 1.394(3), 1.377(4), and 1.393(5) Å, respectively].[9] The asymmetric bonding arrangement in **3a**·OEt_2 is also reflected in a difference of 0.07 Å in the B−N bond lengths of the chelating bam ligand. As expected, the As−N bond involving the four-coordinate nitrogen atom is significantly longer than those involving the three-coordinate nitrogen atoms [As1−N1 = 1.962(2) Å vs As1−N2 = 1.876(2) and As1−N3 = 1.845(2) Å].

The structure of **3c**·OEt_2 exhibits four-coordinate bismuth and lithium centers in a tetracyclic arrangement (Figure 4b). The structural disparity between **3c**·OEt_2 and **3a**·OEt_2 is tentatively attributed to the smaller size of arsenic compared to bismuth, which in conjunction with lithium coordination to three nitrogens, impedes As1−N4 bond formation because of steric repulsions between the ^{t}Bu-groups on N4 and N1. Three of the Bi−N bond lengths in **3c**·OEt_2 span a narrow range [2.239(3)−2.283(3) Å], whereas the fourth contact (Bi1−N4) is ∼0.18 Å longer. Similarly, two of the Li−N

bonds are equal within the experimental error, but the third contact (Li1−N4) is longer by ∼0.23 Å. All Li−N and Bi−N bonds are slightly longer than the single bond length (sum of the covalent radii for Li−N and Bi−N is 1.93 and 2.16 Å, respectively).[25] The average Bi−N bond length in the chelating bam ligand increases significantly along the series **1c**, **2c**, and **3c**·OEt_2 with values of ∼2.13, 2.18, and 2.28 Å, respectively. Lithium coordination results in a significant perturbation (0.07 Å) of the B−N bond lengths in the chelating bam ligand, since N1 is four-coordinate and N2 is three-coordinate, whereas the difference is only ∼0.04 Å in the bam ligand that is coordinated to both Li1 and Bi1.

Variable-Temperature NMR Studies of LiM[PhB(N^{t}Bu)$_2$]$_2$ (3a, M = As; 3b, M = Sb; 3c, M = Bi). The ^{1}H NMR spectrum of **3a** at room temperature shows three singlets in a 1:2:1 intensity ratio for the $C(CH_3)_3$ hydrogens and a multiplet for phenyl hydrogens. Consistently, three singlets in a 1:2:1 ratio are observed in the $^{13}C\{^1H\}$ NMR spectrum for the $C(CH_3)_3$ and $C(CH_3)_3$ carbons, in addition to the characteristic resonances of the phenyl carbons. The ^{7}Li and ^{11}B NMR spectra exhibit singlets at 1.27 and 34.1 ppm, respectively. Since identical resonances are observed after crystallization from either *n*-hexane or diethyl ether, the NMR spectra (measured in toluene-d_8 and in THF-d_8) suggest that the formation of the unsolvated complex **3a** is preferred over the solvated **3a**·OEt_2.

In contrast to the 1:2:1 pattern observed for the $C(CH_3)_3$ hydrogens in the ^{1}H NMR spectrum of **3a**, the ^{1}H NMR spectrum of the isostructural complex **3b** in toluene-d_8 at room temperature displays one broad singlet for the $C(CH_3)_3$ hydrogens. Consistently, singlets are also observed in the $^{13}C\{^1H\}$ NMR spectrum for the $C(CH_3)_3$ and $C(CH_3)_3$ carbons. The ^{7}Li and ^{11}B NMR spectra exhibit singlets at 1.05 and 34.9 ppm, respectively. The observation of a single environment for the $C(CH_3)_3$ groups in **3b** suggests that a fluxional process occurs in solution at 296 K that results in four equivalent ^{t}Bu environments on the NMR time scale.

The room-temperature ^{1}H NMR spectrum of **3c**·OEt_2 in toluene-d_8 shows a singlet for the $C(CH_3)_3$ hydrogens, in addition to the characteristic resonances for Et_2O coordinated to lithium and the phenyl hydrogens. Singlets are also observed for the $C(CH_3)_3$ and $C(CH_3)_3$ carbons in the $^{13}C\{^1H\}$ NMR spectrum. The ^{7}Li and ^{11}B NMR spectra exhibit singlets at 0.19 and 35.1 ppm, respectively. The half-width of the ^{1}H NMR resonance of ^{t}Bu groups for **3c**·OEt_2 is significantly narrower than that observed for **3b** at room temperature (2.14 vs 5.16 Hz) suggesting a faster fluxional process at room temperature.

To gain some insights into the nature of the fluxional processes observed for the bis-bam complexes LiM[PhB(N^{t}Bu)$_2$]$_2$, variable-temperature (VT) ^{1}H NMR studies of **3a**, **3b**, and **3c**·OEt_2 in toluene-d_8 were carried out. This dynamic NMR investigation revealed different behavior for each of the bis-boraamidinates **3a**−**c** in solution. The singlet observed for **3c**·OEt_2 at room-temperature splits into two singlets with

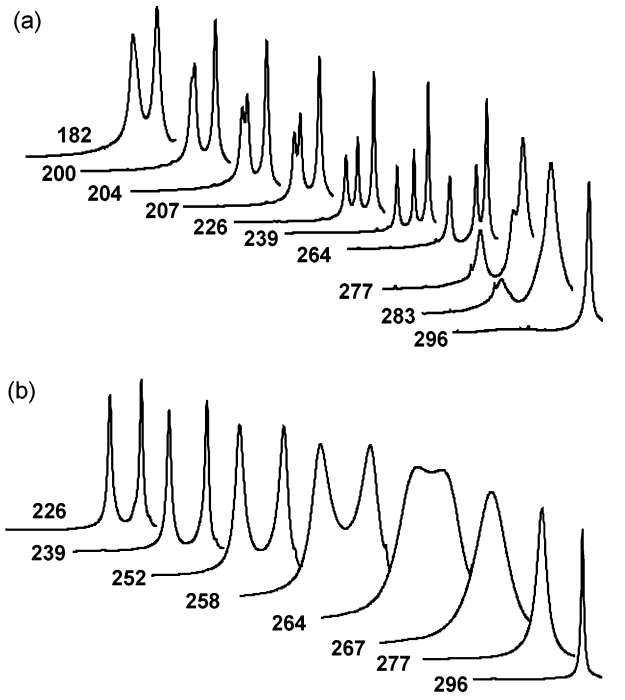

Figure 5. $C(CH_3)_3$ resonances in the VT ^{1}H NMR spectra of (a) LiSb[PhB(N^{t}Bu)$_2$]$_2$ (**3b**) and (b) Li(OEt$_2$)Bi[PhB(N^{t}Bu)$_2$]$_2$ (**3c**·OEt_2). Only selected temperatures (K) are shown.

a 1:1 intensity ratio at 264 K (Figure 5). By contrast, as the temperature is lowered, the broad resonance of **3b** divides first into three singlets with a 1:1:2 intensity ratio at 277 K, and then the two low-field resonances coalesce at 200 K resulting in two singlets with equal intensities. These differences in the VT ^{1}H NMR spectra suggest that two kinetic processes occur for the antimony complex **3b**, whereas only one takes place for the solvated bismuth complex **3c**·OEt_2. In contrast to **3b** and **3c**·OEt_2 and despite the structural similarity between **3a** and **3b** in the solid state, the arsenic complex **3a** exhibits nonfluxionality in solution; the three singlets with a 1:2:1 intensity ratio observed for the $C(CH_3)_3$ groups in the ^{1}H NMR spectrum remain unchanged in the temperature range of 182−334 K.

The fluxional process observed for **3c**·OEt_2 can be explained by a mechanism related to Berry pseudorotation[26] in which the equatorial and axial ^{t}BuN groups of a trigonal bipyramid exchange positions via, ideally, a square pyramidal intermediate while the pivotal position, occupied by the lone pair, remains unchanged. We propose that, at low temperatures (i.e., below the coalescence temperature of 264 K), the two equally intense ^{1}H NMR resonances can be attributed to the axial and equatorial ^{t}BuN groups of the $[Bi(bam)_2]^-$ anion in a trigonal bipyramidal geometry in which the counterion lithium is coordinated to the two equatorial nitrogens (Scheme 2). When the temperature is increased, a fluxional process occurs via intermediate **IIc** in which the solvated lithium ion is coordinated to *three* nitrogens. The proposed pseudo-square pyramidal geometry of the intermediate **IIc** resembles that of the solid-state structure of **3c**·OEt_2 (Figure 4b). At room temperature, a rapid exchange

(25) Pauling, L. *The Nature of the Chemical Bond*, 3rd ed.; Cornell University Press; Ithaca, NY, 1960.

(26) Berry, R. S. *J. Chem. Phys.* **1960**, *32*, 933.

Scheme 2. Fluxional Behavior (Berry Pseudorotation, **I**−**III**) Observed for **3b** and **3c**·OEt_2 in Solution[a]

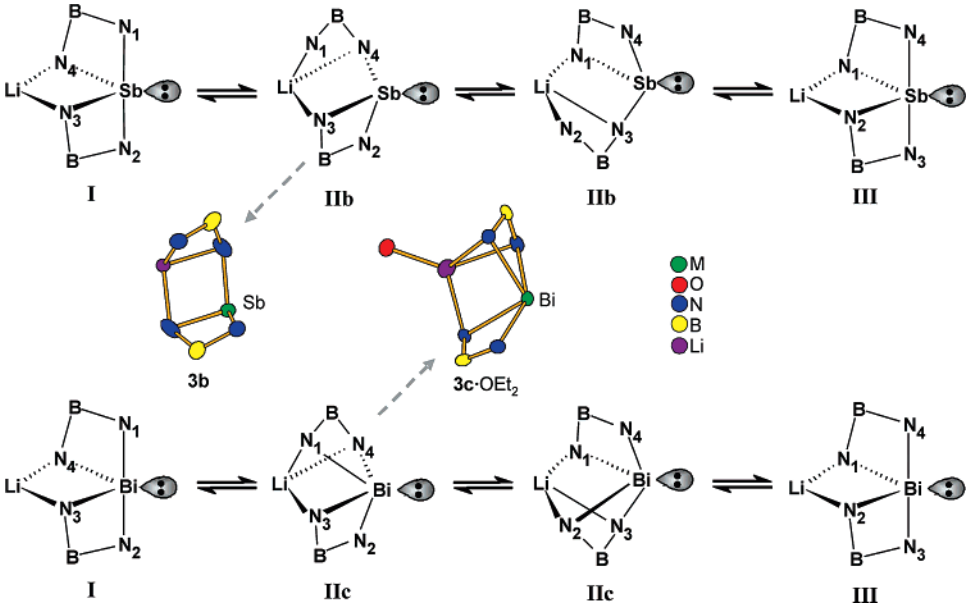

[a] Substituents on B and N and the OEt_2 solvate in **3c**·OEt_2 are omitted for clarity. The dashed arrows indicate the similarity between intermediates **IIb** and **IIc** and the solid-state structures of **3b** and **3c**·OEt_2, respectively.

Table 5. Kinetic Data for $LiSb[PhB(N^tBu)_2]_2$ (**3b**) and $Li(OEt_2)Bi[PhB(N^tBu)_2]_2$ (**3c**·OEt_2)

3b		**3b**		**3c**·OEt_2	
k_1 (s^{-1}, 226 K)	707	k_2 (s^{-1}, 296 K)	170	k (s^{-1}, 296 K)	3.9×10^3
$\Delta H^{\ddagger}_1$ (kJ mol^{-1})	12.0 ± 0.5	$\Delta H^{\ddagger}_2$ (kJ mol^{-1})	80.7 ± 2.7	$\Delta H^{\ddagger}$ (kJ mol^{-1})	76.3 ± 2.9
$\Delta S^{\ddagger}_1$ (J K^{-1} mol^{-1})	-135 ± 3	$\Delta S^{\ddagger}_2$ (J K^{-1} mol^{-1})	72 ± 10	$\Delta S^{\ddagger}$ (J K^{-1} mol^{-1})	80 ± 11

takes place in which the uncoordinated nitrogen center alternates, since all four ^{t}BuN groups are indistinguishable for lithium coordination.

On the basis of the VT NMR data, the fluxional behavior of **3b** appears to be separated into two processes. The observation of two equally intense resonances below 200 K implies a trigonal bipyramidal structure **I** (Scheme 2) similar to that described above for **3c**·OEt_2. To explain the 1:1:2 pattern for the ^{t}BuN group resonances that evolves upon raising the temperature, we propose the formation of the pseudo-square pyramidal intermediate **IIb** in which one of the Sb−N bonds is cleaved. This results in symmetry-related ^{t}Bu groups on nitrogen atoms N_3 and N_4, while the ^{t}Bu groups on N_1 and N_2 are in unique environments. This structure gives rise to the ladderlike arrangement observed for **3b** in the solid state (Figure 3). Similar to that for **3c**·OEt_2, the collapse of these three resonances into a singlet upon a further increase in temperature (above 277 K) is attributed to rapid exchange in which the nitrogen coordination alternate between antimony and lithium centers (Scheme 2).

The arsenic-containing bis-bam **3a** does not exhibit fluxionality in solution, and as in **3b**, the fourth As−N bond is absent in the solid-state structures of **3a** and **3a**·OEt_2. The 1:2:1 pattern observed in the ^{1}H NMR spectrum of **3a** can be attributed to a pseudo-square pyramidal geometry analogous to that of the antimony intermediate **IIb**. The lack of fluxionality in **3a** is attributed primarily to the higher activation enthalpy (for the Berry pseudorotation) caused by the greater steric repulsion that results from the shorter As−N bonds compared to the Sb−N bonds, that is, the tbp geometry with four As−N and two Li−N bonds (**I** and **III** in Scheme 2) is hindered. Similarly, the cleavage of the fourth M−N bond (M = As, Sb) in both **3a** and **3b** is attributed to the steric strain caused by the smaller size of arsenic and antimony compared to bismuth, as was inferred from the comparison of the solid-state structures of **3a**·OEt_2 and **3c**·OEt_2.

The kinetic data for **3b** and **3c**·OEt_2 were analyzed using the line-shape method for rate constant determination, and the enthalpies, $\Delta H^{\ddagger}$, and entropies, $\Delta S^{\ddagger}$, of activation were calculated from the Eyring equation.[27] The results of the analyses are summarized in Table 5, and full details can be found in the Supporting Information. As suggested by the broadness of the ^{1}H NMR singlets at room temperature, the rate of the fluxional process in **3b** is significantly slower than that in **3c**·OEt_2, thus supporting the proposed Sb−N bond cleavage in **3b** ($k_2 = 170$ s^{-1} and $k = 3.9 \times 10^3$ s^{-1} at 296 K for **3b** and **3c**·OEt_2, respectively). The enthalpy of activation for this kinetic process exhibits only a slightly higher barrier for the transition state in **3b** than that in **3c**·OEt_2 ($\Delta H^{\ddagger}_2 = 80.7 \pm 2.7$ kJ mol^{-1} and $\Delta H^{\ddagger} = 76.3 \pm 2.9$ kJ mol^{-1} for **3b** and **3c**·OEt_2, respectively). Values of the entropies and enthalpies of activation for these processes are comparable within the standard deviation, but the opposite enthalpy−entropy balance results in a significant difference between k_2 and k. As expected, the low-temperature process for **3b** (**I** → **IIb**) has a relatively small activation enthalpy

(27) Sandström, J. *Dynamic NMR Spectroscopy*; Academic Press; New York, 1982.

of 12.0 ± 0.5 kJ mol^{-1} indicating a very low energy barrier for the Sb−N bond cleavage and the formation of a third Li−N coordination upon going from **I** to **IIb**. The negative value for the entropy of activation indicates a more ordered arrangement for the transition state between **I** and **IIb**.

The exchange process observed for **3b** and **3c**·OEt_2 is reminiscent of the fluxionality observed in group 13 spirocyclic complexes $Li(OEt_2)M[PhB(N^tBu)_2]_2$ (M = Ga, In), for which only a single ^{t}BuN resonance was observed at room temperature.[9] In those cases, however, VT NMR studies were not conducted. More generally, such fluxional processes in lithium derivatives of polyimido anions of p-block elements have low activation energies.[28]

Conclusions

The versatile coordinating ability of the bam ligand is highlighted in this initial study of heavy group 15 derivatives. The mono-boraamidinates $ClM[PhB(N^tBu)_2]$ (M = As, Sb, Bi) with an M−Cl reactive site are potentially useful reagents for further functionalization of the group 15 element center. The 2:3 bam complexes, $M_2[PhB(N^tBu)_2]_3$ (M = Sb, Bi), display a unique bonding arrangement in which two metal centers are N,N′-chelated by a bam ligand and the two $[M(bam)]^+$ units are bridged by the third $[bam]^{2-}$ ligand. Both solvated and unsolvated structures were observed for the bis-boraamidinates $LiM[PhB(N^tBu)_2]$ (M = As, Sb, Bi). For the arsenic and antimony compounds, the unsolvated complexes exhibit a ladder structure; only the monosolvated complex was isolated for bismuth.

Although the arsenic-containing 1:2 complex **3a** is readily obtained at room temperature, formation of the 2:3 complexes **2b** and **2c** is more favorable than the production of the bis-boraamidinates **3b** and **3c** for antimony and bismuth. The stereochemical activity of the lone pair on the group 15 element center apparently prevents the formation of an arsenic-containing 2:3 bam complex and also contributes to the stereochemical rigidity observed for the antimony and bismuth 2:3 complexes in solution. The influence of the lone pair is also evident in the structures of the bis-boraamidinates, $LiM[PhB(N^tBu)_2]_2$ (M = As, Sb, Bi). Whereas the bismuth complex, $Li(OEt_2)Bi[PhB(N^tBu)_2]_2$, is composed of two chelating bam ligands, the second bam ligand in the arsenic and antimony 1:2 compounds is bonded to both the lithium center and the group 15 element as a result of the shorter M−N bonds and the resulting steric interaction of the ^{t}Bu groups.

The fluxional process observed in solution for **3b** and **3c**·OEt_2 can be explained by a mechanism related to Berry pseudorotation in which axial and equatorial pairs of ^{t}BuN groups exchange via a distorted square pyramidal intermediate. In the case of the antimony-containing bis-bam complex **3b,** two kinetic processes are involved as a result of cleavage of the fourth Sb−N bond during the tbp → square pyramid conversion.

Acknowledgment. The authors gratefully acknowledge financial support from the Academy of Finland (J.K.) and the Natural Sciences and Engineering Research Council (Canada) and thank Dr. Dana Eisler for helpful comments.

Supporting Information Available: X-ray crystallographic files in CIF format, variable-temperature ^{1}H NMR spectra of **3b** and **3c**·OEt_2, and details of the kinetic data analysis. This material is available free of charge via the Internet at http://pubs.acs.org.

IC0622757

(28) Brask, J. K.; Chivers, T. *Angew. Chem., Int. Ed. Engl.* **2001**, *40*, 3960.